



Properties of Discrete-Time Bifurcation-Based Amplifiers

Marco Reit, Sven Feldkord and Wolfgang Mathis

Institute of Theoretical Electrical Engineering, Leibniz Universität Hannover
Appelstraße 9A, D-30167 Hannover, Germany
Email: reit@tet.uni-hannover.de, mathis@tet.uni-hannover.de

Abstract—The remarkable filtering characteristics of the mammalian auditory system inspire scientists and engineers to transfer the underlying signal processing principles into technical applications. An established element in the modeling of the nonlinear amplification processes of the hearing organ is the Hopf-type amplifier, that is based on the resonance behavior near the onset of an Andronov-Hopf bifurcation. Following this idea with focus on a digital realization, we show in this contribution first investigations of the nonlinear input-output characteristic of an amplifier based on the Neimark-Sacker bifurcation in the discrete-time domain. We evaluate common features and differences with respect to parameter dependencies.

1. Introduction

One of the main tasks in engineering sciences is the detection and amplification of weak signals. This is the primary processing step for a large number of sensor applications and measurement systems as well as RF- and wireless communication systems. The challenge often lies in the extraction of small desired signals with certain frequencies from a noisy environment. This requires a filtering characteristic with a strong amplification of faint signals in a narrow frequency band. Moreover, a high dynamic range allows the processing of a wide range of signal levels. As a technical example, the lock-in amplifier is a measurement system to detect weak signals in an extremely narrow frequency band. However, due to its linear amplitude response, it requires advanced electronic circuitry to extend the dynamic range [1]. More efficient examples for the aforementioned tasks can be found in visual and auditory systems in the biology [1]. Especially physiological measurements on the mammalian auditory system have shown that the high dynamic range is achieved by a nonlinear dynamic compression where stronger amplifications appear towards weaker input stimuli [1, 2]. Furthermore, decreasing the input amplitude is associated with a narrower bandwidth [2]. Since it has turned out that this nonlinear amplification characteristic can be described mathematically by using the normal form equation of the supercritical Andronov-Hopf bifurcation [3], several models of the auditory system have been developed [4–8]. Besides the hearing research, the so called Hopf-type amplifier also shows great potential for a variety of other technical applications. Recent investigations clarified all parameter de-

pendencies of the input-output behavior of the Hopf-type amplifier [9–12]. This investigations benefit from the particular feature that a sinusoidal input signal leads to a pure sinusoidal output signal with the same frequency. This allows the calculation of an algebraic equation describing the nonlinear input-output behavior dependent on all given parameters and thus deeper insights in the nonlinear behavior [10–12]. In general, the Hopf-type amplifier is based on the resonance behavior near the onset of the Andronov-Hopf bifurcation. Several realizations of such an amplifier exist [1, 6–8]. Following the Hopf-type amplifier in the continuous-time domain, we investigate in this contribution the resonance behavior of the equivalent Neimark-Sacker bifurcation in the discrete-time domain. We analyze common features and differences with respect to parameter dependencies. Due to its high dynamic range and its coincident input dependent adaptive bandwidth, this novel digital nonlinear amplifier offers new possibilities in digital signal processing.

2. Hopf-Type Amplifier

The generic Hopf-type amplifier is described by the (truncated) normal form equation of the Andronov-Hopf bifurcation. Using the ω_0 -rescaled form [7] and adding the excitation term $a(t)$, the associated differential equation is given by

$$\dot{z} = (\mu + i)\omega_0 z + \sigma\omega_0 |z|^2 z - \omega_0 a, \quad z(t), a(t) \in \mathbb{C}. \quad (1)$$

Here, i is the imaginary unit, $\mu \in \mathbb{R}$ denotes the bifurcation parameter and ω_0 is the natural frequency of oscillation. In general, the coefficient σ is a complex quantity $\sigma = \sigma_R + i\sigma_I$. Omitting the excitation and using the substitution $z(t) = r(t)e^{i\varphi(t)}$ converts (1) into the polar coordinates

$$\dot{r} = \omega_0 r (\mu + \sigma_R r^2), \quad \dot{\varphi} = \omega_0 + \sigma_I \omega_0 r^2. \quad (2)$$

Besides the fixed point at the origin, (2) shows the steady-state solution $r = \sqrt{-\mu/\sigma_R}$. Thus, the amplitude of the self-sustained oscillation depends on the real part of the coefficient σ , in contrast to the oscillation frequency, $\dot{\varphi} = \omega_0 - \mu\omega_0\sigma_I/\sigma_R$, which is affected by both, the real and the imaginary part of σ . Since the system should serve as an amplifier, it must operate in that region, where the stable fixed point is the only solution. This condition is fulfilled by choosing the parameters to $\sigma_R < 0$ and $\mu \leq 0$. In this

case, the system shows a supercritical Andronov-Hopf bifurcation at $\mu = 0$ [13]. Otherwise, for $\sigma_R > 0$ and $\mu \geq 0$, the single fixed point is unstable and the bifurcation is subcritical [13]. The description in polar coordinates (2) shows the rotational symmetry around the equilibrium point $r = 0$. This leads to the assumption, that the sinusoidal input signal $a(t) = a_0 e^{i\omega t}$ in (1) results in the sinusoidal steady-state response $z(t) = z_0 e^{i(\omega t + \varphi)}$. Hence, substituting $a(t)$ and $z(t)$ in (1) allows the calculation of the input-output amplitude relation

$$a_0 = \sqrt{(\mu z_0 + \sigma_R z_0^3)^2 + ((1 - \omega/\omega_0) z_0 + \sigma_I z_0^3)^2}, \quad (3)$$

as well as the phase relation (see [12]). Beside the well studied dependencies of the Hopf-type amplifier response regarding the bifurcation parameter μ as well as the amplitude a_0 and frequency ω of the excitation [3, 6, 7], recent investigations focus on the nonlinearity coefficient σ [9, 11, 12]. The representation of σ by the absolute value $\hat{\sigma}$ and the phase δ as $\sigma = \sigma_R + i\sigma_I = \hat{\sigma} e^{i\delta}$ provides deeper insights in the parameter dependencies of the input-output behavior. The resulting effects on the steady-state response by variation of $\hat{\sigma}$ and δ are shown in Fig. 1. An increase in $\hat{\sigma}$ leads to a compression of the output amplitude z_0 . Hence, $\hat{\sigma}$ denotes a damping factor. The variation of δ leads to a uniform rotation of the resonance structure around the point $(\omega = \omega_0, \mu = 0)$. In this case, for the interval $\pi/2 < \delta < 3\pi/2$ the Andronov-Hopf bifurcation is of supercritical type. As shown by the dashed line at the cross section $\mu = -0.1$, the variation of δ causes hysteresis effects in the input-output behavior, that have already been studied for certain relations between σ_R and σ_I [9, 11]. With these results, the parameter dependent input-output behavior is fully understood.

3. Bifurcation-Type Amplifier Realizations

Further investigations of the response behavior of the Hopf-type amplifier to more complicated transient input stimuli first motivates the realization of cochlea specific signal processing principles by means of electronics. Software simulations possess the drawback that solving nonlinear differential equations with high accuracy is time consuming and needs high computing power. Since recently, attention has focused on the nonlinear amplification characteristics of the Hopf-type amplifier, electronic realizations also become attractive for applications. One of those areas refers to hearing aids, where the constraints are on the one hand real-time processing with low latency and on the other hand low power consumption. These conditions also hold for other mobile applications like RF- and wireless communication systems. Another application field are sensors and measurement systems, in which the accuracy and dynamic range are the key parameters. In dependency of the scope of application and its regarded conditions, it must be chosen between an analog, digital or mixed-signal

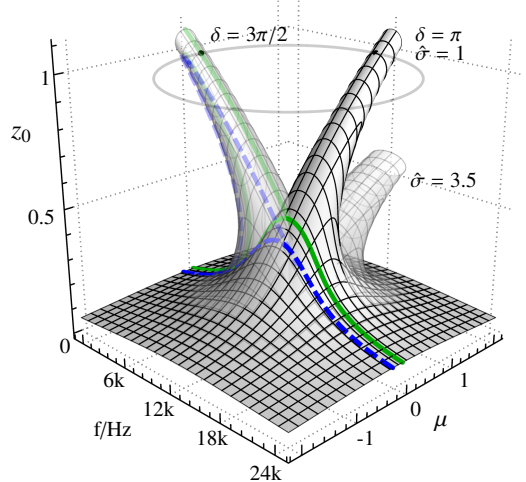


Figure 1: Steady-state response of the Hopf-type amplifier by variation of $\hat{\sigma}$ and δ . Excitation amplitude $a_0 = 0.1$, characteristic frequency $\omega_0 = 2\pi \cdot 12$ kHz ($\omega = 2\pi f$). Intersection lines for $\mu = 0$ (solid) and $\mu = -0.1$ (dashed).

realization. The first analog electronic Hopf cochlea circuit was build up using discrete electronic components, such as operational amplifiers, multipliers, capacitors and resistors to emulate the differential equation by means of analog computing [6, 7]. Shortly after that, a Hopf-type amplifier was built up using a LCR loop with a chain of diodes as the essential nonlinear element [1]. Since this analog circuit represents a kind of van der Pol oscillator, we assume high harmonic distortions based on our investigations [10]. To overcome the drawbacks of an analog realization, for instance the variation and noise of the electronic components, no tunable parameters or only in terms of voltages, external electrical couplings etc., we constructed a first highly flexible and scalable digital realization implemented on a digital signal processor [8]. The main objectives were real-time processing with low latency and low power consumption [8]. Therefore, we choose the explicit 4th-order Runge-Kutta method to compute (1) with a good compromise between accuracy and performance [8]. The digital processing of the Hopf-type amplifier always underlies damping and stability issues depending on the integration method. Thus, we investigate in this contribution the resonance behavior of the Neimark-Sacker bifurcation in the discrete-time domain, which is referred to as the Andronov-Hopf bifurcation for maps [13].

4. Neimark-Sacker-Type Amplifier

The normal form of the Neimark-Sacker bifurcation [13] with an added excitation term p is described by the map

$$z \mapsto e^{i\theta} z (1 + \gamma + \sigma |z|^2) + p, \quad z, p \in \mathbb{C}. \quad (4)$$

Here, $\sigma = \sigma_R + i\sigma_I = \hat{\sigma} e^{i\delta}$ is the nonlinearity coefficient and γ is the bifurcation parameter. For a discrete-time

system with an equidistant time interval, the angle θ can be considered as normalized characteristic frequency $\theta = 2\pi\omega_0/\omega_s = 2\pi f_0/f_s$ with the characteristic frequency of the system f_0 and the sampling frequency f_s , ($\omega = 2\pi f$). The bifurcation behavior is similar to the Andronov-Hopf bifurcation in the continuous-time domain. Omitting the excitation, the map (4) shows for $\sigma_R < 0$ a supercritical bifurcation at $\gamma = 0$ where a stable closed invariant curve grows for $\gamma > 0$ from a stable fixed point $\gamma \leq 0$ which changes its stability at $\gamma = 0$ [13]. Otherwise, for $\sigma_R > 0$ and $\gamma < 0$ a stable fixed point is surrounded by an unstable closed invariant curve that vanishes by subcritical bifurcation at $\gamma = 0$ where an unstable fixed point remains for $\gamma > 0$ [13]. The bifurcations occur, when the complex-conjugate pair of eigenvalues of (4), which calculates to $\lambda_{1,2} = e^{\pm i\theta}(1 + \gamma)$, crosses the unit circle at $\gamma = 0$ [13]. Moreover, the eigenvalues also crosses the unit circle at $\gamma = -2$. The characteristics of this latter bifurcation become obvious by substituting the translation $\tilde{\gamma} = -2 - \gamma$ into (4), that results in

$$z \mapsto e^{i\tilde{\theta}}(1 + \tilde{\gamma} - \sigma|z|^2)z + p, \quad z, p \in \mathbb{C}, \quad (5)$$

with $\tilde{\theta} = \theta \pm \pi(2n + 1) = 2\pi(f_0 \pm (n + 1/2)f_s)/f_s$, $n \in \mathbb{N}_0$. Thus, the sign of the coefficient σ inverts, which causes a change between the supercritical and subcritical bifurcation behavior. Additionally, the characteristic frequency of the bifurcation shifts in terms of the half sampling frequency. In general, since we are dealing with a discrete-time system, the characteristic frequencies of the bifurcations are periodic with the sampling frequency. This refers equally to θ in (4) which can be written in the more general form $\theta = 2\pi(f_0 \pm n f_s)/f_s$, $n \in \mathbb{N}_0$. Here, it should be emphasized that for the reconstruction of a continuous-time signal, the Nyquist–Shannon sampling theorem must be hold. Since the map (4) is rotationally symmetric, we assume for $-1 \leq \gamma \leq 0$ that a sinusoidal input signal $p_n = p_0 e^{in\beta}$ leads to the sinusoidal output signal $z_{n+1} = z_0 e^{i((n+1)\beta + \varphi)}$, here n denotes the iteration variable. Normalization of the signals on the sampling frequency $\beta = 2\pi\omega/\omega_s = 2\pi f/f_s$ and substituting in (4) allows to calculate the input-output amplitude relation

$$p_0^2 = z_0^2 \left(2 + (\sigma_R^2 + \sigma_I^2) z_0^4 + (2 + \gamma)\gamma + 2\sigma_R(1 + \gamma) z_0^2 - 2(1 + \gamma + \sigma_R z_0^2) \cos(\beta - \theta) - 2\sigma_I z_0^2 \sin(\beta - \theta) \right), \quad (6)$$

as well as the phase relation, which is neglected at this point. The algebraic equation (6) describes the amplitude z_0 of the output signal caused by a sampled sinusoidal excitation dependent on all given parameters in (4). This allows parametric studies to get deeper insights of the input-output behavior of the Neimark-Sacker-type nonlinear amplifier.

In order to analyze common features and differences against the Hopf-type amplifier in section 2, the resulting output amplitude z_0 is plotted over the excitation frequency f and the bifurcation parameter γ as illustrated in Fig. 2. Compared to the output amplitude of the Hopf-type am-

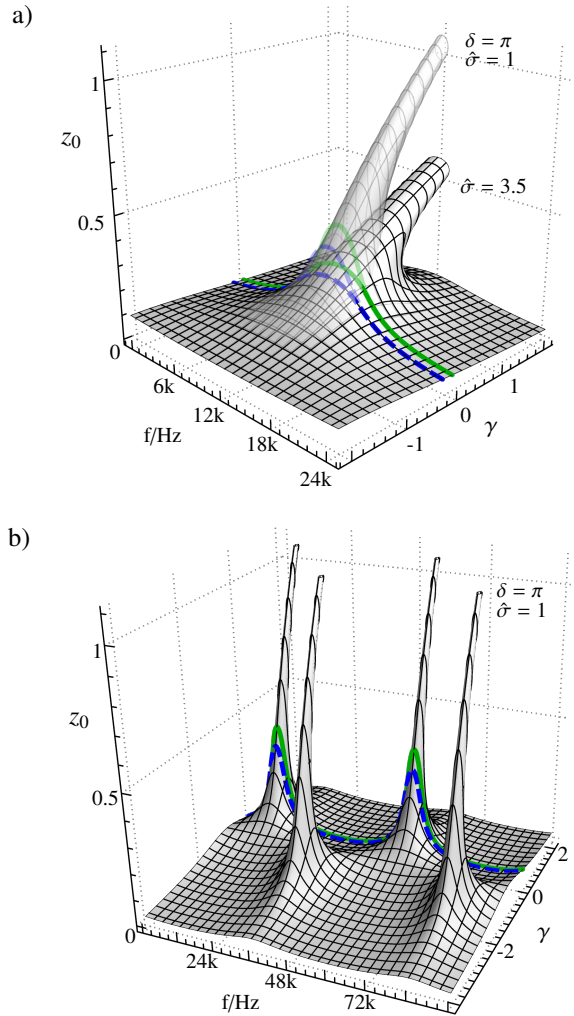


Figure 2: Steady-state response of the Neimark-Sacker-type amplifier. Excitation amplitude $p_0 = 0.1$, characteristic frequency $f_0 = 12$ kHz, sampling frequency $f_s = 48$ kHz and $\sigma_I = 0$. Intersection lines for $\mu = 0$ (solid) and $\mu = -0.1$ (dashed). Variation of $\hat{\sigma}$ in a), wider range of the excitation frequency and parameter γ with $\sigma_R = -1$ in b).

plifier in Fig. 1, huge similarities in the input-output behavior can be noted. Figure 2a) shows, that the amplification increases by shifting the bifurcation parameter towards the bifurcation point $\gamma = 0$. Additionally, $\hat{\sigma}$ also denotes a damping factor. Considering a broader range for the excitation frequency f and the bifurcation parameter γ in Fig 2b) points out, that (6) includes the aforementioned periodicity of the resonance structures in terms of the sampling frequency as well as the resonance structure of the subcritical Neimark-Sacker bifurcation at $\gamma = -2$ shifted by $f_s/2$. Here, it must be noted that the frequency range of discrete-time systems consists of frequencies between $-f_s/2$ and $f_s/2$. Thus, analytic signals with a frequency f in the range of $f_s/2 < f < f_s$ are mapped to analytic signals with the frequency $\tilde{f} = f - f_s$ in the range of negative

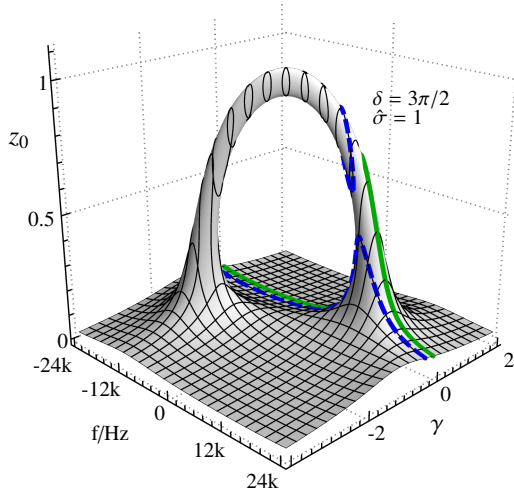


Figure 3: Steady-state response of the Neimark-Sacker-type amplifier. Excitation amplitude $p_0 = 0.1$, characteristic frequency $f_0 = 12$ kHz, sampling frequency $f_s = 48$ kHz and $\sigma_I = -1$, $\sigma_R = 0$. Intersection lines for $\mu = 0$ (solid) and $\mu = -0.25$ (dashed).

frequencies $-f_s/2 < \tilde{f} < 0$, where the output amplitude and the resonance structure is still the same due to the f_s -periodicity. The same applies for frequencies lower than $-f_s/2$ vice versa. To analyze the influence of the imaginary part of σ and to compare the behavior with the Hopf-type amplifier in Fig 1, we plot the output amplitude z_0 of the Neimark-Sacker system in Fig. 3 while using $\sigma_R = 0$ and $\sigma_I = -1$. It is shown, that the behavior strongly differs. Besides the rotation, a bending and connecting of the sub- and supercritical resonance structures occur, which always exists for $\sigma_I \neq 0$. The dashed intersection line at $\mu = -0.25$ discloses, that additionally to the hysteresis behavior, separated solution sets arise. In general, this kind of ambiguities are hard to find by numerical simulations or measurements.

5. Conclusion

In this work, we investigate a nonlinear amplifier that is based on the normal form equation of the Neimark-Sacker bifurcation in the discrete-time domain. Following the idea of the Hopf-type amplifier, we can derive algebraic equations that describe the parameter dependent input-output behavior regarding the properties of the discrete-time domain. This allows parametric studies which disclose ambiguities in form of hysteresis effects and separated solution sets. Since the amplification characteristic shows huge similarities to the Hopf-type amplifier, it could be preferred to a digital realization of the latter one by means of an integration method, which underlies damping and stability issues as well as higher calculation effort. Our analysis gives deeper insights in the input-output behavior of a bifurcation-based amplifier in the discrete-time domain.

References

- [1] N.J. McCullen, T. Mullin, M. Golubitsky, “Sensitive Signal Detection Using a Feed-Forward Oscillator Network”, *Phys. Rev. Lett.*, vol. 98, 254101, 2007.
- [2] M.A. Ruggero, “Responses to Sound of the Basilar Membrane of the Mammalian Cochlea”, *Curr. Opin. Neurobiol.*, vol. 2, pp. 449–456, 1992.
- [3] V.M. Eguíluz, M. Ospeck, Y. Choe, A. Hudspeth, M. Magnasco, “Essential Nonlinearities in Hearing”, *Phys. Rev. Lett.*, vol. 84, 5232, 2000.
- [4] S. Camalet, T. Duke, F. Jülicher, J. Prost, “Auditory Sensitivity Provided by Self-Tuned Critical Oscillations of Hair Cells”, *Proc. Natl. Acad. Sci.*, vol.97 no.7, 3183–3188, 2000.
- [5] K.A. Montgomery, M. Silber, S.A. Solla, “Amplification in the Auditory Periphery: The Effect of Coupled Tuning Mechanisms”, *Phys. Rev. E*, vol.75, 051924, 2007.
- [6] J.-J. van der Vyver, A. Kern, and R. Stoop, “Active Component Implementation of a Biomorphic Hopf Cochlea”, *Proc. European Conference on Circuit Theory and Design*, vol.3, 285-288, 2003.
- [7] R. Stoop, T. Jasa, Y. Uwate, S. Martignoli, “From Hearing to Listening: Design and Properties of an Actively Tunable Electronic Hearing Sensor”, *Sensors*, vol.7, 3287–3298, 2007.
- [8] M. Reit, W. Mathis, R. Stoop, “Time-Discrete Nonlinear Cochlea Model Implemented on DSP for Auditory Studies”, *Nonlinear Dynamics of Electronic Systems, Proceedings of NDES 2012*, pp.1–4, 2012.
- [9] Y. Zhang, M. Golubitsky, “Periodically Forced Hopf Bifurcation”, *SIAM J. Appl. Dyn. Syst.*, vol.10 no.4, 1272–1306, 2011.
- [10] M. Reit, R. Stoop, W. Mathis, “Analysis of Cascaded Canonical Dissipative Systems and LTI Filter Sections”, *Acta Technica*, vol.59 no.1, 79-96, 2014.
- [11] M. Reit, W. Mathis, “A Class of Sinusoidal Driven Nonlinear Input-Output Systems with Sinusoidal Response”, *Proceeding of International Symposium on Nonlinear Theory and its Applications (NOLTA)*, 2014.
- [12] M. Reit, M. Berens, W. Mathis, “Ambiguities in Input-Output Behavior of Driven Nonlinear Systems Close to Bifurcation”, *Archives of Electrical Engineering*, vol.65 no.2, 2016.
- [13] Y. A. Kuznetsov, “Elements of Applied Bifurcation Theory”, *Springer Science & Business Media*, vol.112, 2013.